A FAST AND EFFECTIVE APPROACH TO MODELLING SOLAR ENERGY POTENTIAL IN COMPLEX SHADING ENVIRONMENTS

I.R. Cole*, D. Palmer, T.R. Betts & R. Gottschalg

CREST
Loughborough University
LE11 3TU
UK

*Corresponding Author: I.R.Cole@lboro.ac.uk, +44 (0)1509 635605

ABSTRACT: A fast and effective model for the computation of solar energy potential in complex shading environments is presented. Accurate calculation and identification of solar energy potential profiles is demonstrated over large areas. Calculation time is exceptionally fast, even on an average specification PC (typically under 1 min per 1 km^2). Problems with commonly used low-resolution sky domes that can lead to irradiance calculation errors of ~5% are identified. Ideal placements are easily visually identified from resultant irradiance/irradiation profile images. Image processing techniques for spatially distributed optimization problems are described and an example of energy value optimization is presented by means of individual dwelling demand separation & comparison.

Keywords: see enclosed list of keywords

1 MOTIVATION

The deployment of rooftop photovoltaic (PV) systems has seen rapid expansion in recent years, vastly exceeding predictions. The UK scenario is presented for reference in Figure 1 [1]. Almost all of these systems are grid connected, supplying electricity to the national grid when not consuming it on site. There is no definable pattern to the geographic distribution of these installations and information on the vast majority of these systems is not documented, yet alone accessible.

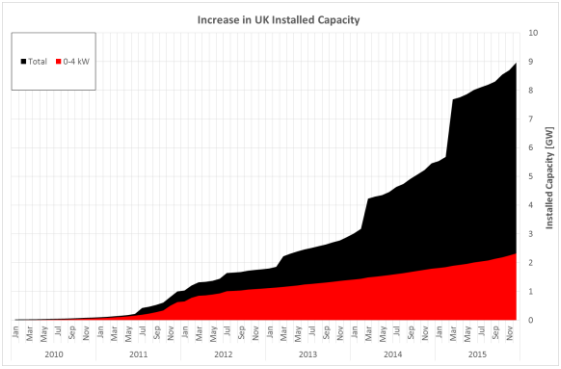

Figure 1: UK PV Deployment from 2010 to 2016 by Capacity [1]

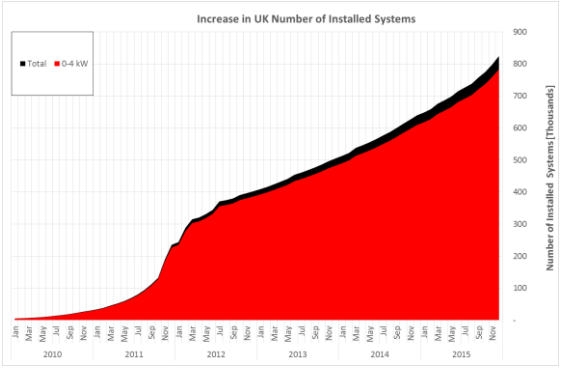

Figure 2: UK PV Deployment from 2010 to 2016 by Count [1]

In built up areas especially, optimisation of the deployment of PV is a non-trivial task. Shading can have a depredatory effect on system performance and, with residential installations in particular, system owners are often ill equipped to identify performance issues. Furthermore, at the system design or fault identification stages, the person time involved in the assessment of installation conditions by surveying is often prohibitively expensive, particularly for large scale applications.

Figure 3 demonstrates a relevant issue of note. A citywide set of approximately 2000 PV system installations in Nottingham, UK, show performances relative to the expected mean that are negatively skewed. Shading and sub-optimal installation conditions are likely significant contributors to this skew.

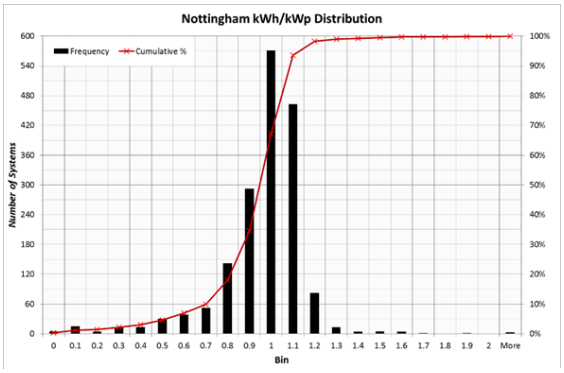

Figure 3: Performance spread of installed systems in Nottingham, UK, as indicated by kWh/kWp values normalised to a 'standard' system

Example problem installations are shown in Figure 4 and Figure 5. Unfortunately, these examples are two of many and represent a significant problem in rooftop system installations.

Figure 4: Building to Building Shading System Example (Credit: Nigel Monk, CREST)

Figure 5: Shading by a Nearby Tree Example (Credit: Brian Goss, CREST)

This work presents and describes a model, solarscene.xyz. The purpose of this model is to automate the identification of optimum and poor installation conditions, mitigating the problems described above.

2 MODEL DESCRIPTION

2.1 Objective

There exist a number of tools to accelerate system design and decision making processes. These tools do not typically include coherent shading analysis, but do offer a commonplace infographic to help designers arrive at the optimum installation angle for a given location. This is a relative energy harvest for varying installation angles, the equivalent as generated by solarscene.xyz is given in Figure 6.

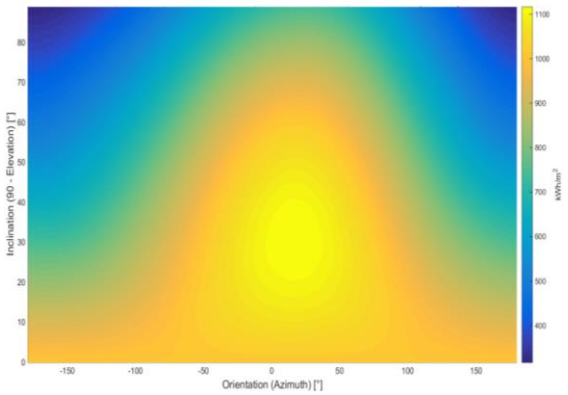

Figure 6: Net annual solar irradiation collection dependency on module orientation and inclination for Sutton Bonnington, UK, in 2014

Such information offers a useful guide for choice of PV farm module orientation or in the identification of suitable roofs in situations where there is next to no light obstruction and data is available on roof orientation. However, it is rarely the case that much is known about roof designs and vectors for wide scale applications and gathering such information can be both time consuming and costly. Furthermore, particularly in built-up areas, light obstruction is commonplace.

The key objective of this model was to generate a map of spatially distributed irradiation collection that can be used to easily identify optimum installation locations as well as potential problem areas. This has been achieved. An example of such a map compared to a Google Maps image of a given location is shown in Figure 7.

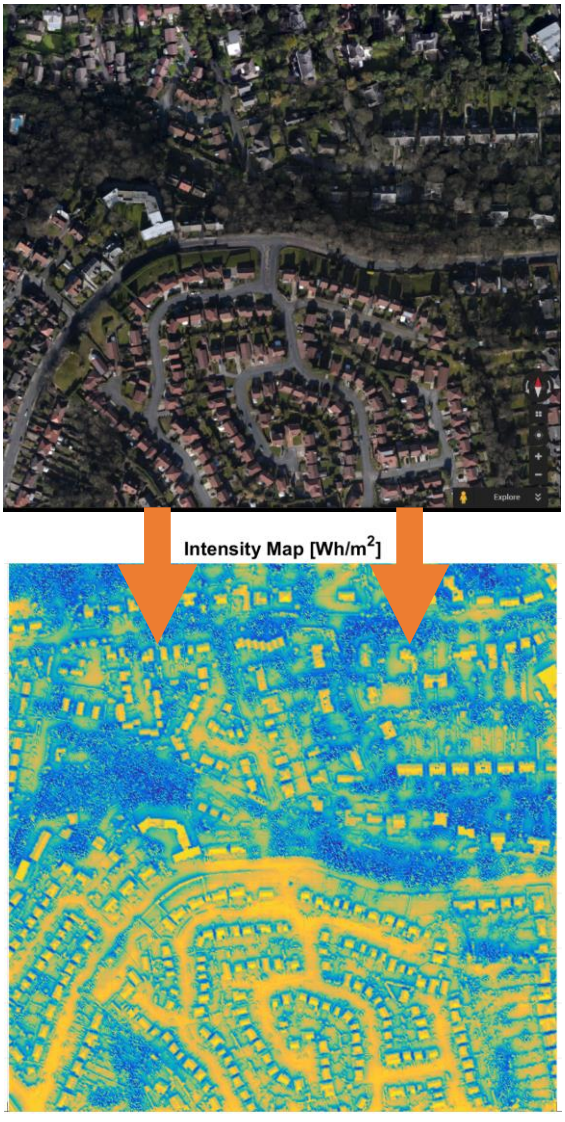

Figure 7: Net annual solar irradiation collection for each pixel in a 0.25 km² LiDAR map of Prestwich, UK, for 2014 using interpolated Met Office irradiation data

A secondary objective of the model was to be computationally efficient and to run in little time on an average specification PC. This has also been achieved, the above map took under 10 s to generate.

2.2 Model Description

The model can be considered in three distinct stages, as shown in Figure 8. Input data describing the environment is split into mapped 3D data describing the terrestrial surface and meteorological data describing the local weather variations. These input data are processed and passed through to a ray trace algorithm which generates mapped solar energy data. Each phase is described separately in this section.

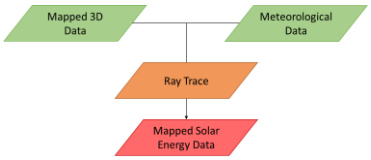

Figure 8: Model Flowchart

3D Environment Data

The input 3D environment primary data is in the form of a map of pixel heights. Metadata map layers are also used for specific analysis, for example, highlighted regions of interest can be used to provide specific focus to output data. Test case data from LiDAR has been used here for illustration. CAD drawings of proposed building plans or .stl conversions are also possible. It is also possible to place a proposed building plan within a set of LiDAR (or other existing) data to construct a contextualised placement scenario.

An interpolated surface is produced from the input LiDAR points mesh. This surface is used to form surface normal vectors from each pixel that are used in intensity correction calculations. Here, a mesh resolution of 1 m^2 was used. The mesh resolution is variable and is dependent on user requirements/available data. A one km^2 example is presented in Figure 9, the region presented is the same as that shown in Figure 7, expanded is the northerly and easterly directions.

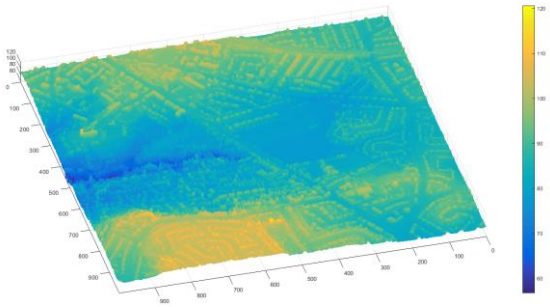

Figure 9: Points to Surface Map from LiDAR – 1 km^2 of Prestwich, UK

A cuboidal columnar representation of the data is also created (Figure 10). It is this surface that is used in the ray trace analysis for shading profile calculation and is key to the computational efficiency of the simulation.

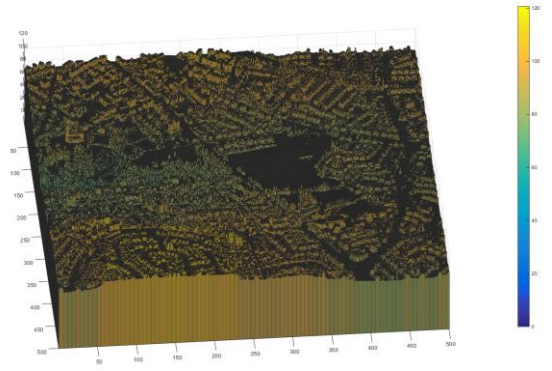

Figure 10: Points to Cuboidal Columnar Map from LiDAR – 1 km^2 of Prestwich, UK

Meteorological Data

Input meteorological data is in the form of horizontally received beam and diffuse irradiation. The temporal resolution of this is variable, depending on user requirements and available data. Currently, the model does not use albedo irradiation as there is little data available for this. However, this is planned as an extension in future development of this model. The irradiance values used here have been derived by weighted interpolation of met office hourly irradiation values for nearby and neighbouring sites.

The irradiance/irradiation (in instantaneous/ time-extended analyses) is distributed within a hemispherical representation of the sky, termed a sky dome (Figure 11). Each segment of the sky dome is individually traced through the 3D environment and the contribution of its power/energy to each surface pixel calculated as a multiplication of its value, shading factor and angle of incidence correction.

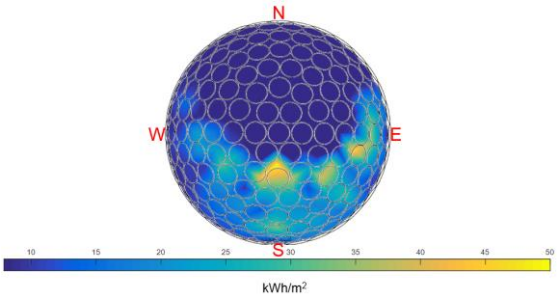

Figure 11: Net Annual Sky Dome Example with Tregenza Overlay

This tool was developed at CREST for the generation of high resolution maps of solar energy potential for existing and/or proposed (building plans) locations. These calculated solar energy potential maps include global and localised shading effects. Time resolved output maps allow for the specific investigation of shading scenarios, rather than limiting the results to averaged values. Diffuse and beam irradiance components are specifically considered and the model is easily extended to include spectral effects.

For ease of presentation, Figure 11 uses a common segmentation of the sky into 151 patches known as the Tregenza dome [2]. In practice, use of the Tregenza dome is not acceptable for energy prediction scenarios as the granularity of the dome, especially regarding elevation, causes unnatural stepped values in in-plane irradiance, as

shown in Figure 12. These can lead to errors in calculated irradiance values of ~5%,

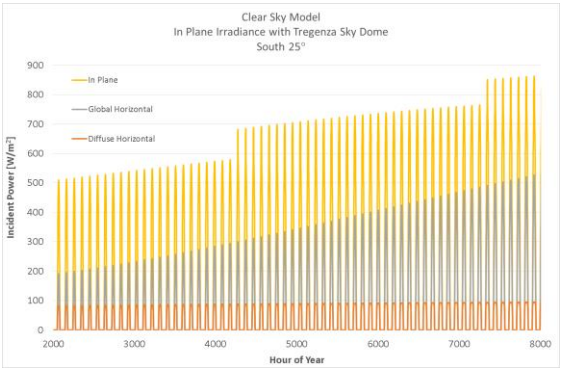

Figure 12: Stepped In-plane Irradiance Artefacts from Low Resolution Sky Dome

Alternative sky domes derived by similar means are presented in [3], although in practice any sky dome of suitable resolution (mitigating the artefacts shown in Figure 12) can be used. The relative contribution of diffuse irradiance can corrected for by calculating the relative projected area contribution of the confined surface by, for example, Equation 1. The selection of an appropraitely defined sky dome can also lead to a significant increase in computational efficiency in the sky patch location of sun position.

$$\int_{\gamma_{s_1}}^{\gamma_{s_2}} \int_{h_1}^{h_2} \cos h \, . \, dh \, . \, d\gamma_s$$

Equation 1

Where γ_s is the solar azimuth angle and h the solar elevation angle (see [4] for explanation of terms)

Ray Trace Method

The ray trace method employed here is one developed at CREST, building on the work presented in [5-7]. Comparisons with existing methods such as [8 & 9] are presented in [10]. The procedure is optimised for the specific calculations performed here. This is a marked advantage over using off-the-shelf solutions as any data beyond that required is simply not calculated here, rather than computed and not used. Much computational time is thus saved in this approach. Further to the streamlined computation process, the ray trace procedure here is divided in 16 special cases: the four major compass directions, the four minor compass directions and the 8 spaces between Figure 13. The case is first identified and the corresponding optimised calculation procedure triggered in the code accordingly.

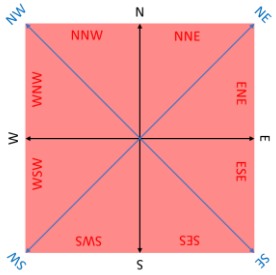

Figure 13: Compass Directions Broken Into 16 Special Cases for Efficient Computation

Using this method, the net annual irradiation values on each 1 m^2 pixel in a 1 km^2 region using hourly meteorological data distributed in a Tregenza dome can be calculated on an average specification PC in under 1 min. A further optimisation advantage to this method is that relative map trace values for a given location and sky dome combination can be stored and later recalled for investigation of a different meteorological dataset – bypassing the ray trace procedure altogether – at which point the computational time reduces to a value that is primarily dependent on data drive read/write speeds.

3 MODEL PERFORMANCE & UTILIZATION

3.1 Validation

The most visually significant validation for the key model objective is a comparison of model shadow identification with those visible from aerial photography. Here, for clarity, the 0.25 km^2 image of Figure 7 is used. Figure 14 shows the shading pattern produced by the model. It can be seen that the resultant shadows are extremely well aligned. The corresponding sun position used in this instantaneous test case is shown in Figure 15.

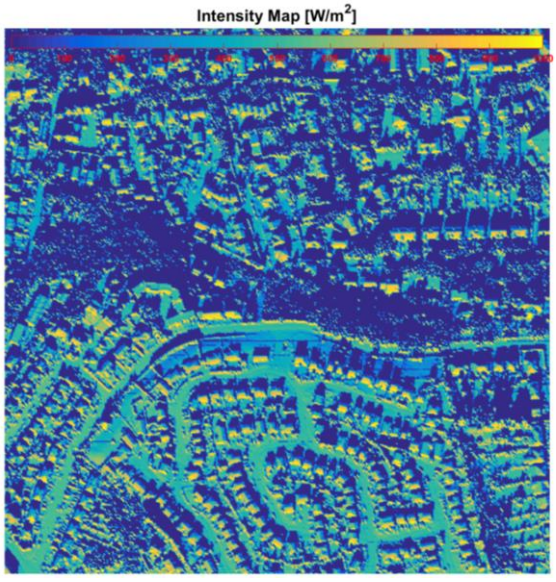

Figure 14: Intensity Map Produced by solarscene.xyz Showing Matching Shadow Profiles (see Figure 7)

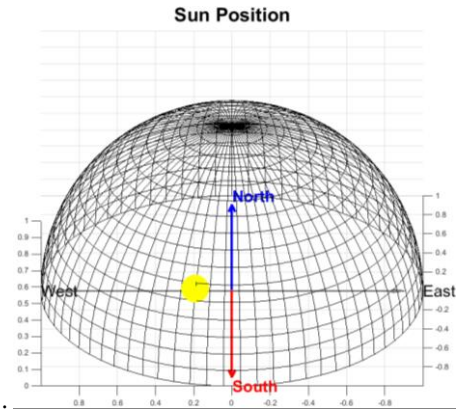

Figure 15: Depiction of the Sun Position used in the Generation of Figure 14

It is these instantaneous profiles that are integrated in order to obtain the primary model objective – irradiation maps, as shown in Figure 7.

3.2 Model Utilization

With further processing of the images generated by the model or the use and analysis of related spatially distributed information, the model can be further developed as a tool for optimization problems. Two example model developments that are currently being explored are shown below.

Automated Identification of Optimum Installation Locations – Preliminary Investigation

It can clearly be seen from Figure 7 that certain areas are significantly brighter than others. If the image is generated in greyscale then the brightness of each pixel is directly related to an annual irradiation value. Thus this lends itself particularly well to an image processing for analysis.

Figure 16 shows the process of taking a given location, generating a greyscale irradiation map, applying a threshold brightness filter to extract pixels above 700 W/m^2 and then applying a morphological filter (2 m*4 m rectangle) to determine a space suitable for solar panel installation. This process will be further developed and published in future work.

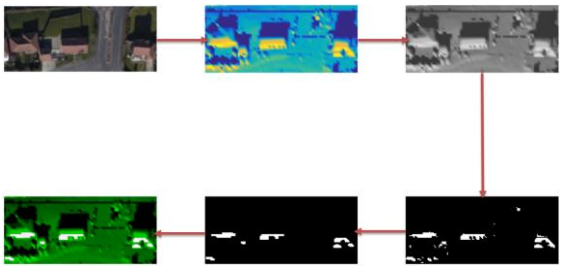

Figure 16: Image Processing for Optimum Installation Location Determination - Preliminary Example

Relative Value by Dynamic Assignment – Preliminary Investigation

The irradiation map presented in Figure 7 is useful in the context of optimization or energy harvest. However, the reality of energy value is dynamic. For example, peak generation time of south facing residential rooftop PV systems at 12:00 is mostly wasteful. A simple investigation of energy value optimization is shown below. Figure 17 shows normalized energy harvest for a given location, with only rooftop pixels shown for a 200 m by 200 m area in Nottingham, UK.

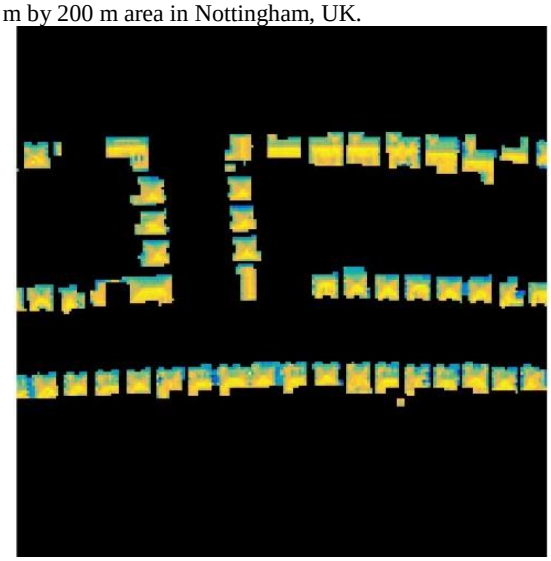

Figure 17: Normalised Irradiation Harvest on Nottingham Rooftops

Data separating each individual dwelling was then obtained and 5 realistic energy usage profiles were generated using [11]. These profiles are shown in Figure 18.

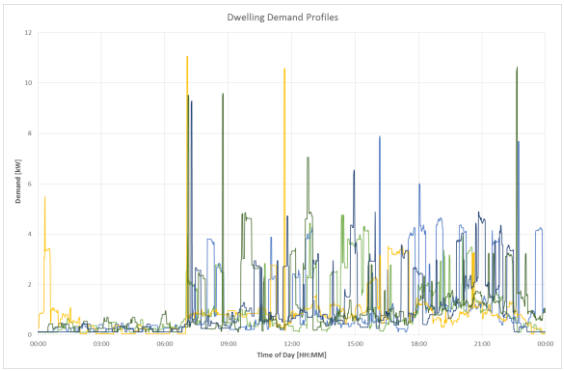

Figure 18: 5 Different Example Energy Demand Profiles

The simulation was then rerun, randomly assigning one of the 5 demand profiles to each of the dwellings above and producing a normalised map of energy value per pixel (see Figure 19). The resultant map is significantly different to Figure 17. This will be investigated further and published in future work.

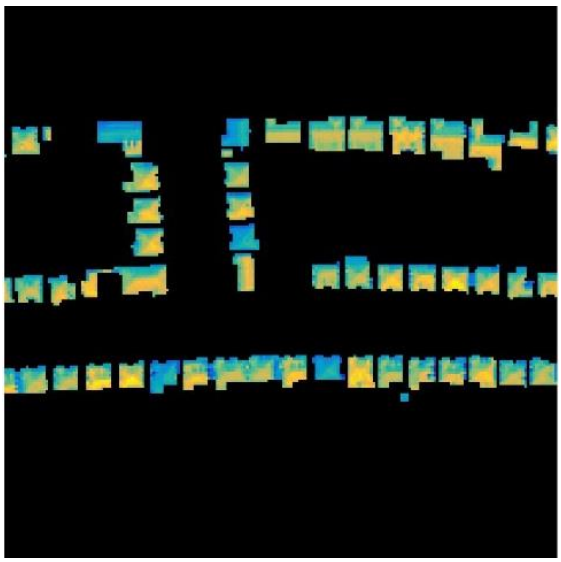

Figure 19: Normalised Energy Value on Nottingham Rooftops

4 CONCLUSIONS

- A Fast and Effective Approach to Modelling PV Potential in Complex Shading Environments has been Developed and Presented.
- Accurate Pixel by Pixel Irradiance and Irradiation Maps Are Calculated by the Model
- Key mistakes in existing models have been Identified (Can Lead to ~5% Irradiance Calculation Error)
- The Automated Identification of Optimum Installation Conditions has been Demonstrated
- The Identification of Potential Problem Areas and System Underperformance due to Shading has been Demonstrated

There will be much further development of this model. Some opportunities for development have been identified here alongside preliminary investigations, though there are many more possibilities for useful model expansion and utilization. solarscene.xyz will be made publically available later in the year. The authors welcome collaborative works and feedback.

5 REFERENCES

[1] National Statistics – Solar photovoltaic deployment, Department of Energy and Climate Change (DECC), UK Government, 25 February 2016

[2] TREGENZA, P. R. 1987. Subdivision of the sky hemisphere for luminance measurements. Lighting Research and Technology, 19 (1), 13-14.

[3] GOSS, B., COLE, I., BETTS, T. & GOTTSCHALG, R. 2014. Irradiance modelling for individual cells of shaded solar photovoltaic arrays. Solar Energy, 110, 410-419.

[4] ISO 9488:1999 – Solar Energy – Vocabulary

[5] COLE, I. R., BETTS, T. R. & GOTTSCHALG, R. 2012. Solar Profiles and Spectral Modeling for CPV Simulations. IEEE Journal of Photovoltaics, 2, 62-67.

[6] COLE, I. R. & GOTTSCHALG, R. 2015. Optical Modelling for CPV Systems: Insolation Transfer Variations with Solar Source Descriptions. IET Renewable Power Generation, 9, 412-419.

[7] COLE, I. R. & GOTTSCHALG, R. 2016. Improved Model for Circumsolar Irradiance Calculation as an Extended Light Source and Spectral Implications for High-Concentration Photovoltaic Devices. IEEE Journal of Potovoltaics, 6(1), 258-265.

[8] BERGAMASCO, L., & ASINARI, P. 2011. Scalable methodology for the photovoltaic solar energy potential assessment based on available roof surface area: Further improvements by ortho-image analysis and application to Turin (Italy), Solar Energy, 85, 2741–2756.

[9] TARINI, M., CIGNONI, P. & MONTANI, C. 2006. Ambient Occlusion and Edge Cueing to Enhance Real Time Molecular Visualization, IEEE Transactions on Visualization and Computer Graphics, 12(5), 1237-1244.

[10] PALMER, D., GOSS, B., COLE, I., BETTS, T. & GOTTSCHALG, R. 2015. Detection of Roof Shading for PV Based on Lidar Data Using a Multi-Modal Approach. Proceedings of the 31st Photovoltaic Solar Energy Conference, 1753 – 1759.

[11] Richardson, I and Thomson, M (2012) Integrated simulation of photovoltaic micro-generation and domestic electricity demand: a one-minute resolution open-source model, Proceedings of the Institution of Mechanical Engineers, Part A: Journal of Power and Energy, -, DOI: 10.1177/0957650912454989.